Frequency response of unified dielectric and conductive systems involving an exponential distribution of activation energies

J. Ross Macdonald
Department of Physics and Astronomy, University of North Carolina, Chapel Hill, North Carolina 27514

(Received 22 August 1984; accepted for publication 15 May 1985)

When the small-signal ac frequency response of a dielectric or conductive system is known, either functionally or as data, it is shown that the corresponding response of an associated conductive or dielectric system may be immediately obtained through the use of new duality relations. A specific model is considered which involves thermally activated capacitance and/or resistance, with an activation energy probability density exponentially dependent on energy. Previous frequency response analyses of such a continuously distributed model involve inadequate approximations and lead to erroneous predictions. Correct immittance results are presented in three ways: analytically, by means of complex plane plots, and through the use of three-dimensional perspective plots. Results are given in general form but apply to both dielectric and conductive systems which involve the same functional dependence on activation energies. Low- and high-frequency-limiting responses for a given system are found to be associated with the same simple equivalent circuit. In intermediate frequency ranges a power-law frequency response somewhat like that of the constant phase element may occur. Differences between the power-law exponents for dielectric and conductive systems are clarified, and the types of possible temperature dependence of the exponents explored. Exponent values are not limited to the range between zero and unity. The overall response of the present normalized three-parameter model is similar to that often found experimentally for both dielectric and conductive systems and similar to but more general than that of other normalized distributed-element (two-parameter) models such as that of Williams and Watts and that of Davidson and Cole.

I. INTRODUCTION

Work in the area of continuously distributed activation energies began with the paper[1] of Gevers and du Pré who assumed that relaxation times of a dielectric system were thermally activated and a given relaxation time τ could thus be written as

$$\tau = \tau_p \exp(E/kT), \tag{1}$$

where E is the appropriate activation energy. They then introduced the concept of a continuous distribution of activation energies (DAE), leading to a continuous distribution of relaxation times (DRT). For the amorphous materials in which they were interested, they essentially took the DAE function, a probability density, as a constant, independent of E. They then discussed the frequency response of the system following from approximate treatment of the integrals involved. At the same time, Garton[2] also examined the DAE situation in order to find under what conditions it could lead to a nearly frequency-independent $\epsilon''(\omega)$, where the complex dielectric constant $\epsilon \equiv \epsilon' - i\epsilon''$ and $i \equiv \sqrt{-1}$. Such dependence for ϵ'' has often been observed experimentally. He found, after various approximations, that again a DAE function independent of activation energy was required.

Next, Macdonald[3] showed that most of the usual DRT functions, including those of Cole and Cole,[4] and Davidson and Cole,[5] were inconsistent with a DAE. Although every DAE is associated with a DRT, most DRT's are not consistent with a DAE. Yet it is often more probable that a DAE is present and leads to a DRT than that the preexponential factor τ_p alone is distributed and yields a DRT. Further work of Nowick and Berry[6] and Macdonald[7] considered various combinations of independent and dependent distributions of τ_p and E. The present author[8] discussed the important case where $\tau_p \equiv \tau_{p0} \exp(S/k)$ and the entropy S and the activation energy (actually enthalpy) E were taken as possibly linearly related, with their distributions arising from that of a common structure factor. Such a relationship between E and S is often found experimentally.[9,10]

The first exact treatment of a specific DAE situation with a plausible choice for the activation energy probability density function seems to be that of Ref. 9, which dealt entirely with transient response and found t^{-n} behavior over a wide range of t, where t is the time variable and the exponent n was found to have a specific form of temperature dependence. A somewhat similar yet entirely independent treatment later led to the same dependence.[10] Time dependence of the above sort has often been observed for a wide variety of dielectric-material experimental situations,[9-11] usually with $0 < n \leq 1$.

The next significant work is that of Dutoit *et al.*[12] and Laflère *et al.*[13] who did not refer to the earlier work of Refs. 3 and 6–9. These authors developed a dielectric-system DAE treatment to explain the frequency dependence observed for various semiconductor/electrolyte interfaces. This dependence was of the form

$$\mathrm{Re}(Z) = b + a\nu^{-n}, \tag{2}$$

where a and b were independent of frequency ν and they found $1 < n < 2$. Here Z is the measured impedance of the system. It is worth noting that this is just the response to be

 0021-8979/85/171955-16$02.40

expected from a frequency-independent resistor and a constant phase element (CPE) in series.[4,14] When the CPE admittance is written in its usual forms as

$$Y_{\rm CPE} \equiv A_0(i\omega)^n \equiv (i\omega\tau_0)^n = A_0\omega^n[\cos(n\pi/2) + i\sin(n\pi/2)], \quad (3)$$

with $\omega \equiv 2\pi\nu$, one usually expects $0 \leqslant n \leqslant 1$, however.

Now in Ref. 9 I assumed that the specific DAE probability density function was of the form

$$F(E) = N\exp(-\eta_j E), \quad (4)$$

or, equivalently,

$$F(\mathscr{E}) = N\exp(-\lambda_j \mathscr{E}), \quad (5)$$

where N is a normalization constant, $\mathscr{E} \equiv E/kT$, and $\lambda_j \equiv kT\eta_j$. I have simplified the results here by identifying the structure factor directly with E. Two different λ_j's were defined for different parts of the $\mathscr{E}_0 \leqslant \mathscr{E} \leqslant \mathscr{E}_\infty$ range over which $F(\mathscr{E})$ was taken to be nonzero. The choice of an exponential probability density was somewhat justified in Ref. 9; it is analogous to the introduction of a set of traps distributed exponentially in energy below the conduction band in semiconductor work; and it is made more plausible by some of the considerations of Ref. 15. Further, several of the DAE's derived from transient response data on protein systems[10] are approximately of the form of Eq. (5) for a finite $\mathscr{E}$ range. Although exponential dependence is an assumption, it is further justified in the transient response case by being the only form of a DAE which leads to the experimentally observed t^{-n} response. For the present work I shall again use this form but without the added generality of two λ_j's and so will take a single $\lambda_j \equiv \lambda$. Results following from the more general choice will be investigated in later work.

An exponential DAE was assumed without comment in the Dutoit and Laflère work,[12,13] where they took a single λ and implicitly assumed $\mathscr{E}_0 = 0$ and $\mathscr{E}_\infty = \infty$. To carry out their analysis they required $-1 < \lambda < 0$. But taking λ negative, so the probability density increases with increasing $\mathscr{E}$ over the entire range to $\mathscr{E} \to \infty$ is physically impossible, although it is not impossible for a finite range of $\mathscr{E}$. For this reason we have written Eqs. (4) and (5) with negative exponent signs and will usually restrict attention to the $\lambda \geqslant 0$ case.

Although Dutoit and Laflère indeed obtained frequency response of the $a\nu^{-n}$ form of Eq. (2) from their analysis, they stated that their results were restricted to the low-frequency range, $\omega\tau \ll 1$. But because of their $E_\infty = \infty$ choice, their results actually only apply for $\omega \equiv 0$ and are therefore not useful (see Appendix A). For these reasons a correct and more general analysis of DAE frequency response with the of $F(\mathscr{E})$ of Eq. (5) and $\lambda_j \equiv \lambda$ is needed and is provided below.

But first, there is a further valuable paper which largely followed the Refs. 12 and 13 approach but introduced an important new element. Specifically, McCann and Badwal[16] split the thermally activated τ of Eq. (1) into two parts through the relation $\tau \equiv RC$ and took both R and C separately thermally activated. In the present notation they thus wrote

$$R = R_a\exp(\alpha\mathscr{E}) \quad (6)$$

and

$$C = C_a\exp(\beta\mathscr{E}), \quad (7)$$

where α and β were taken temperature independent. McCann and Badwal were concerned with a DAE associated with a continuous distribution of thermally activated elemental R's and C's in series and thus implicitly treated what we shall identify here as a dielectric system. Now τ may be written as

$$\tau \equiv RC = \tau_a\exp(\gamma\mathscr{E}), \quad (8)$$

where

$$\gamma \equiv \alpha + \beta, \quad (9)$$

$\tau_a \equiv R_aC_a$, and all quantities with "a" subscripts are taken frequency and temperature independent.

McCann and Badwal made the same approximations and $E_0 = 0$, $E_\infty = \infty$ assumptions as those in Refs. 12 and 13 and, in addition, implicitly took $\lambda = 0$, thus taking the same probability density for the full $0 \leqslant E \leqslant \infty$ range. This is the same constant DAE function originally used by Garton.[2] With the $\lambda = 0$ choice, McCann and Badwal obtained frequency response of the form of a CPE, Eq. (3), though their results were not so identified. When one combines the limiting ranges for n found separately for the real and imaginary parts of their theoretical admittance, it is found that $0 < n < 1$. But again their results actually apply only for $\omega \equiv 0$ (see Appendix A).

It is often expected and frequently found that all, or the dominant part, of the thermal activation of τ arises from that of R, with little or no temperature dependence of C. There are instances, however, where the temperature dependence of both R and C is of importance and β is not ≈ 0. For example, consider the electrolyte double layer situation where the reaction capacitance, i.e., the diffuse double-layer capacitance, is proportional to $c_0^{1/2}$ and the reaction resistance is proportional to c_0^{-1}. Here c_0 is the bulk concentration of the electroactive mobile charged species. If c_0 is itself thermally activated and we consider temperature effects arising only from such activation, then we may set $\alpha = 1$ in Eq. (6) and $\beta = -0.5$ in Eq. (7), so $\gamma = 0.5$. We shall consider only the $\gamma > 0$ situation in most of the rest of the paper.

In the following work we present an exact analysis which corrects and generalizes the work of Refs. 12, 13, and 16, show how a common approach may be used for conductive as well as dielectric systems, and examine and plot the various frequency responses predicted by the theory. In addition, present predictions are compared with those of other distributed-element models; limiting high- and low-frequency equivalent circuits are derived for DAE dielectric and conductive systems; and an approach to DAE system data analysis is outlined.

II. SYSTEM RESPONSE: DEFINITIONS AND RELATIONS

There are four frequency-response immittance functions which have been found useful in the analysis and measurement of the electrical response of solid and liquid materials under small-signal conditions. In addition to the impedance, $Z \equiv Z' + iZ''$, admittance, $Y \equiv Y' + iY''$, and complex dielectric constant, $\epsilon \equiv \epsilon' - i\epsilon''$, we may define the complex modulus function $M \equiv M' + iM'' \equiv i\omega C_c Z$, where

TABLE I. Relations between the four basic immittance functions. Here $\mu \equiv i\omega C_c$.

	M	Z	Y	ϵ
M	M	μZ	μY^{-1}	ϵ^{-1}
Z	$\mu^{-1}M$	Z	Y^{-1}	$\mu^{-1}\epsilon^{-1}$
Y	μM^{-1}	Z^{-1}	Y	$\mu\epsilon$
ϵ	M^{-1}	$\mu^{-1}Z^{-1}$	$\mu^{-1}Y$	ϵ

C_c is the capacitance of the measuring cell without the material of interest in it. Now let $\mu \equiv i\omega C_c$. Then the matrix of Table I shows all the interrelations between the four basic immittance functions. For example, we see that $M = \epsilon^{-1}$.

Clearly if theoretical or experimental results are obtained on a given model or system, e.g., the i system, at one of the four levels, say Z_i, then the M_i, Y_i, and ϵ_i results for this system immediately follow from the Table I relations. But now we want to discuss some connections which may be established between the response of a given system and that of its different but associated system. Suppose, for example, that theoretical or experimental results (frequency-response function or data) are available at the Z level, defining Z_Z and thus the Z system itself through its response. Then, of course, M_Z, Y_Z, and ϵ_Z may be immediately calculated. On the other hand, consider ϵ-system results yielding $M_\epsilon, Z_\epsilon, Y_\epsilon$, and ϵ_ϵ. If the Z_Z and ϵ_ϵ measurements were actually all on the same physical system, then of course $Z_\epsilon = Z_Z$, etc. Now it turns out that given either Z_Z *or* ϵ_ϵ (or M_M or Y_Y), a duality transformation applied after suitable dimensionless normalization allows one to obtain an ϵ_ϵ response (and thus M_ϵ, Z_ϵ, and Y_ϵ) from Z_Z and *vice versa*. Of course the resulting $Z_\epsilon \neq Z_Z$ since these reponses now refer to different systems, but the systems themselves are related or correlated by the connecting duality relations. The same sort of connections allow M-system response to be obtained from Y-system response and *vice versa*. These important results imply that given frequency response (for a specific material-electrode system) of *any* functional or experimental form, a new and different frequency response is implied and may be calculated for a different but associated system.

So what? It turns out that these relations prove very helpful in, for example, allowing one general theoretical treatment to yield results for two different but allied systems. Further, all previously known ϵ-system theoretical models, for example, immediately yield possibly useful related Z-system models. We shall illustrate these matters in the following for specific Z- and ϵ-system results of particular experimental interest. Let us define a conductive system (C system) as one whose intrinsic dc conductivity is nonzero. It still remains a C system when, e.g., blocking electrodes or series blocking capacitors are added. If it actually exhibits nonzero intrinsic dc conductivity, it may be termed an ideal C system. Alternatively, define a dielectric system (D system) as one which exhibits no intrinsic dc conductivity. It remains a D system even when a dc path (e.g., a parallel resistor) is added to it, but if there is no such path, it may be termed an ideal D system. These two types of systems and system response have been widely studied for many years but not always with a clear distinction made between them since a general C system may show no actual dc conductivity and a general D system may show some. A C system is most simply defined at the Z level and a D system at the ϵ level. In the following work we shall show how general D-system results imply associated general C-system ones and then will carry out a general DAE analysis which includes both ideal C- and D-system response.

III. ANALYSIS

A. Distributed dielectric system

Let us now define a distributed D system as one in which the elemental unit is a resistance and capacitance in series. In more general terms, the resistance element is associated with the presence of energy dissipation and the capacitance element with the presence of energy storage. Both processes are present in relaxing systems. There are, in the continuous limit, an infinite number of these units in parallel. Thus such a system has no dc conductance as long as no elemental C's are infinite. Similarly we may define a distributed C system as one in which the elemental units are each composed of a resistance and capacitance in parallel, with an infinite number of such differential units in series. Such a system may have a nonzero dc conductance as long as no elemental resistances are infinite. We shall distinguish between quantities calculated for the two different types of systems by using a subscript D for the dielectric one and a subscript C for the conductive system.

These parallel and series structures, where the order of RC elements is immaterial, have hierarchical counterparts which can yield the same overall impedance-frequency response as the parallel or series ones. Thus, they cannot be distinguished from each other by small-signal ac measurements at constant temperature. Of course, for the hierarchical or ladder network structures the ordering of the elements is definitive. We can associate with the parallel structure a hierarchical ladder network made up of series C's and parallel R's; both have zero dc response. Similarly, with the series structure, we can associate a ladder network made up of series R's and parallel C's; here both circuits conduct at zero frequency. Although frequency response for these pairs can be identical, the connectivity of the elemental physical processes involved on a microscopic level is quite different for the two members of a pair. For example, hierarchical structure may be associated with fractal behavior and parallel structure with many independent parallel paths. Although the following work involves parallel and series continuously distributed structures, the above discussion shows that the overall macroscopic results, but not the microscopic processes leading to them, can be considered to represent either parallel or series structures or their associated hierarchical counterparts.

Let us initially consider a nonideal D system. The admittance Y for a single R and C in series and all in parallel with a conductance G_x, Y_D, may be written

$$Y_D = i\omega C/(1 + i\omega RC) + G_x. \tag{10}$$

We may now write for the complex dielectric constant ϵ_D associated with Y_D,

$$\epsilon_D = Y_D/(i\omega C_c) = (C/C_c)/(1 + i\omega RC) + (G_x/i\omega C_c), \tag{11}$$

Here $C/C_c \equiv \epsilon_0$, the $\omega \to 0$ value of ϵ'_D when G_x is zero or is removed. But we see that for $\omega \to \infty$, Eq. (11) yields $\epsilon'_D = \epsilon_\infty = 0$. Thus for more generality we need to introduce a nonzero ϵ_∞. We shall assume that the ϵ_∞ for the dielectric system is not associated with a DRT or DAE. Then the more general ϵ_D may be written as

$$\epsilon_D = (C_\infty/C_c) + [(C_0 - C_\infty)/C_c]/[1 + i\omega R(C_0 - C_\infty)] + (G_x/i\omega C_c), \tag{12}$$

where $C_\infty/C_c \equiv \epsilon_\infty$. We may now consider a distributed system based on Eqs. (6), (7), and (12) and introduce the DRT function $\mathscr{G}_D(\tau)$ by writing

$$\epsilon_D = \epsilon_\infty + C_c^{-1} \int_0^\infty \frac{C\mathscr{G}_D(\tau)d\tau}{1 + i\omega RC} + (i\omega\tau_{Dx})^{-1}, \tag{13}$$

where $\tau_{Dx} \equiv C_c/G_x$. In a pure DRT treatment, in which C is taken independent of τ, the C term in the numerator could be removed from under the integral sign in the usual way,[11] but for the present DAE analysis this would be improper. Correct $\omega \to 0$ limiting behavior of $[\epsilon_D - (i\omega\tau_{Dx})^{-1}]$ can be ensured by selection of the normalization factor included as a part of $\mathscr{G}_D(\tau)$. In a more general case, the single-time-constant $(i\omega\tau_{Dx})^{-1}$ quantity in Eq. (13) might be replaced by a continuously distributed C-system DAE term, yielding a parallel combination of D and C system responses.

Many different heuristic DRT expressions have been suggested for $\mathscr{G}_D(\tau)$, e.g., Refs. 1–7, 9, 11, 17, and 18. The one of most relevance to the present work is[11]

$$\mathscr{G}_D(\tau) = A\tau^{-n}, \tag{14}$$

where A is a constant and $\mathscr{G}_D(\tau)$ is taken zero outside the range $\tau_0 \leqslant \tau \leqslant \tau_\infty$. The DRT frequency response following from using this expression in Eq. (13), with C independent of τ and $G_x = 0$, has been investigated by Matsumoto and Higasi.[17] When one considers a DAE, however, and uses the relation $\mathscr{G}_D(\tau)d\tau = F_D(\mathscr{E})d\mathscr{E}$, which follows from conservation of probability, one finds that Eq. (14) for $\mathscr{G}_D(\tau)$ and Eq. (8) for τ lead[9] to a $F_D(\mathscr{E})$ of just the form of Eq. (5). Thus there is a close connection between the DRT work of Ref. 17, the present DAE analysis, and that of Ref. 9. It is also worth remarking that the $\mathscr{G}_D(\tau)$ DRT expression of Eq. (14) is just that which leads to CPE response when the τ range is taken as $0 \leqslant \tau \leqslant \infty$. But an important defect of the CPE is that it and its DRT are not normalizable.[11] See Appendix A.

For the DAE case, we shall assume that R and C are both associated with the same DAE. On transforming the variable in Eq. (13) from τ to $\mathscr{E}$ and using Eqs. (5), (6), (8), and (12), one finds

$$\epsilon_D = \epsilon_\infty + \left(\frac{C_a N_D}{C_c}\right) \times \int_{\mathscr{E}_0}^{\mathscr{E}_\infty} \frac{\exp[(\beta - \lambda)\mathscr{E}]d\mathscr{E}}{1 + i\omega\tau_a \exp[\gamma\mathscr{E}]} + (i\omega\tau_{Dx})^{-1}. \tag{15}$$

Here N_D is the D-system value of the normalization factor N of Eq. (5). As shown, the finite range $\tau_0 \leqslant \tau \leqslant \tau_\infty$ assumed for τ leads to the range $\mathscr{E}_0 \leqslant \mathscr{E} \leqslant \mathscr{E}_\infty$ over which $F_D(\mathscr{E})$ is nonzero. There is, of course, no mathematical reason why $\mathscr{E}_0$ may not be set to zero although this choice makes $\tau_0 = \tau_a$. On the other hand, the integral of Eq. (15) will only converge when $\mathscr{E}_\infty = \infty$ for $(\beta - \lambda) < 0$.

It turns out that Eq. (15) may be appreciably simplified if we define

$$W \equiv \tau/\tau_0 \equiv \exp[\gamma(\mathscr{E} - \mathscr{E}_0)] \tag{16}$$

and

$$s \equiv \omega\tau_0 \equiv \omega\tau_a \exp(\gamma\mathscr{E}_0), \tag{17}$$

where s is a normalized frequency variable. Note that $\omega RC \equiv \omega\tau \equiv sW$. One then obtains

$$\epsilon_D = \epsilon_\infty + [C_a N_D \gamma^{-1} \exp(\phi_D \gamma \mathscr{E}_0)/C_c] \times \int_1^r \frac{W^{\phi_D - 1}\,dW}{1 + isW} + (is\tau_{Dx}/\tau_0)^{-1}, \tag{18}$$

where

$$\phi_D \equiv (\beta - \lambda)/\gamma = (\beta - \lambda)/(\beta + \alpha), \tag{19}$$

and

$$r \equiv W_\infty \equiv \tau_\infty/\tau_0 \equiv \exp[\gamma(\mathscr{E}_\infty - \mathscr{E}_0)]. \tag{20}$$

For $r \to \infty$ the integral only converges for $\phi_D < 0$. At $s = 0$, we require $[\epsilon_D - (is\tau_{Dx}/\tau_0)^{-1}] = \epsilon_0$, the zero-frequency-limiting value of ϵ' for an ideal D system. This condition allows us to evaluate the normalization factor N_D, assuming that ϵ_0 is a known parameter. One finds

$$\epsilon_D = \epsilon_\infty + (\epsilon_0 - \epsilon_\infty)[\phi_D/(r^{\phi_D} - 1)] \times \int_1^r \frac{W^{\phi_D - 1}\,dW}{1 + isW} + (is\tau_{Dx}/\tau_0)^{-1}, \tag{21}$$

which yields proper $s \to 0$ and $s \to \infty$ limits. Finally let us write

$$I_D \equiv \kappa_D \equiv (\epsilon_D - \epsilon_\infty)/(\epsilon_0 - \epsilon_\infty) = [\phi_D/(r^{\phi_D} - 1)] \int_1^r \frac{W^{\phi_D - 1}\,dW}{1 + isW} + (isQ_D)^{-1}, \tag{22}$$

where I_D is a normalized immittance, here the normalized complex dielectric constant κ_D, equal to unity at $s = 0$ when $Q_D \equiv (C_0 - C_\infty)/(\tau_0 G_x) = \infty$ or is removed.

Now although the admittance Y_D associated with ϵ_D is given by $i\omega C_c \epsilon_D$, it will be convenient to define the normalized admittance Y_{DN} as

$$Y_{DN} \equiv is\kappa_D, \tag{23}$$

which excludes the $C_\infty \equiv C_c\epsilon_\infty$ contribution. Let us also only consider ideal D systems from now on and thus take $Q_D = \infty$. We shall use the subscript "N" to denote that a quantity normalized to unity at $s = 0$ is involved, but for simplicity will omit it from I_i and κ_D. The $s \to \infty$ limit of Eq. (23) is just

$$Y_{DN\infty} = Y'_{DN\infty} = [\phi_D/(\phi_D - 1)][(r^{\phi_D - 1} - 1)/(r^{\phi_D} - 1)]. \tag{24}$$

The electrical circuit associated with ϵ_D thus involves a capacitance C_∞ in parallel with a distributed element whose $s \to 0$ limit is the capacitance $(C_0 - C_\infty)$ and whose $s \to \infty$ limit is a conductance given by $(\omega/s)C_c(\epsilon_0 - \epsilon_\infty)Y'_{DN\infty}$. This high-frequency conductance may therefore be written as

$$G_{D\infty} = R_{D\infty}^{-1} = [(C_0 - C_\infty)/\tau_0]\, Y'_{DN\infty}. \quad (25)$$

Pertinent low- and high-frequency-limiting equivalent circuits are considered in more detail in the final section. Although the distributed ideal dielectric system properly yields no dc conductance, it will generally be dominated at sufficiently high frequencies by the conductance $G_{D\infty}$. The results shown in Eqs. (22), (24), and (25) are only meaningful for $r = \infty$ when $\phi_D < 0$ since Eq. (18) for an ideal D system cannot be normalized when $r = \infty$ unless $\phi_D < 0$. Problems in previous work arising from taking $r = \infty$ with $\phi_D \geqslant 0$ will be discussed later and in Appendix A. We shall consider the behavior of κ_D for the region $0 \leqslant s \leqslant \infty$ in Sec. IV.

B. Distributed conductive system

Although the following treatment is closely analogous to that in the last section, it has not been carried out in the present way before and leads to results different from but related to those above. We start by considering the impedance of a single R and C in parallel, all in series with a blocking capacitor C_x,

$$Z_C = R/(1 + i\omega RC) + (i\omega C_x)^{-1}. \quad (26)$$

In analogy with the treatment of a distributed dielectric system, let us here consider a nonideal C system with a nondistributed high-frequency-limiting resistance R_∞ and a distributed element in series with R_∞ whose zero-frequency-limiting value with the $(i\omega C_x)^{-1}$ term removed or zero is $(R_0 - R_\infty)$. The $\omega \to 0$ limit of Z_C for the full ideal C system is thus R_0, assumed given. We can now write an equation analogous to Eq. (13) involving the conductive-system DRT function[11] $\mathscr{G}_C(\tau)$ as

$$Z_C = R_\infty + \int_0^\infty \frac{R\mathscr{G}_C(\tau)d\tau}{1 + i\omega RC} + (i\omega C_x)^{-1}; \quad (27)$$

again the R term in the numerator must not be taken outside the integral if a DAE is present. On substituting Eqs. (6) and (7) into Eq. (27) and writing $\mathscr{G}_C(\tau)d\tau = F_C(\mathscr{E})d\mathscr{E} = N_C \exp(-\lambda\mathscr{E})d\mathscr{E}$ with F_C only nonzero in the interval $\mathscr{E}_0 \leqslant \mathscr{E} \leqslant \mathscr{E}_\infty$, one finds

$$Z_C = R_\infty + (R_a N_C) \times \int_{\mathscr{E}_0}^{\mathscr{E}_\infty} \frac{\exp[(\alpha - \lambda)\mathscr{E}]d\mathscr{E}}{1 + i\omega\tau_a \exp(\gamma\mathscr{E})} + (i\omega C_x)^{-1}. \quad (28)$$

For $\mathscr{E}_\infty = \infty$, $[Z_C - (i\omega C_x)^{-1}]$ only converges for $(\alpha - \lambda) < 0$. Let us now introduce as before the W, s, and r definitions into Eq. (28), obtaining

$$Z_C = R_\infty + [R_a N_C \gamma^{-1} \exp(\phi_C \gamma \mathscr{E}_0)] \times \int_1^r \frac{W^{\phi_C - 1}\, dW}{1 + isW} + (isC_x/\tau_0)^{-1}, \quad (29)$$

where

$$\phi_C \equiv (\alpha - \lambda)/\gamma = (\alpha - \lambda)/(\alpha + \beta). \quad (30)$$

For $r \to \infty$ the integral without the C_x term only converges for $\phi_C < 0$. The normalization factor N_C may be obtained from the condition $[Z_C - (isC_x/\tau_0)^{-1}] = R_0$ for $s = 0$. Further, let us introduce the normalized immittance I_C defined in the same way as the I_D of Eq. (22). Then,

$$I_C \equiv Z_{CN} \equiv (Z_C - R_\infty)/(R_0 - R_\infty) = [\phi_C/(r^{\phi_C} - 1)] \int_1^r \frac{W^{\phi_C - 1}\, dW}{1 + isW} + (isQ_C)^{-1}, \quad (31)$$

where $Q_C \equiv C_x(R_0 - R_\infty)/\tau_0$. Note that when the single-time-constant Q_C term is replaced by a continuously distributed D-system DAE term, one obtains normalized response which is a *series* combination of D- and C-system DAE responses.

C. Combined systems

Comparison of Eqs. (22) and (31) shows that they are of exactly the same form and become equal if $\phi_C = \phi_D$ and $Q_C = Q_D$. We do not, in fact, need exact equality here in order to apply the duality relation mentioned earlier which connects Z and ϵ systems and responses; equality of form is sufficient. Let the subscript $i = C$ or D; then a general equation for the general I_i function equivalent to Eqs. (22) or (31) may be immediately written which involves ϕ_i and Q_i. This equation yields both D- and C-system DAE response and can be further generalized, as mentioned above, to represent the combined response of a D system and C system in parallel or in series. From now on, for simplicity we shall consider only ideal pure system response and thus take $Q_D = Q_C = \infty$. Then we may write

$$I_i(s,\phi_i) = [\phi_i/(r^{\phi_i} - 1)] \int_1^r \frac{W^{\phi_i - 1}\, dW}{1 + isW}, \quad (32)$$

where ϕ_i is either ϕ_D or ϕ_C. Unfortunately, the integral of Eq. (32) cannot be expressed in closed form for arbitrary ϕ_i. It is possible, however, to so express it for various specific fractional and integral values of ϕ_i. Appendix B summarizes results for $\phi_i = 3/2$, 1, 2/3, 1/2, 1/3, 0, and $-1/2$. This series could be further extended at both ends if desired. For values of ϕ_i for which no closed form is known, one must resort to numerical integration. Although I_i is actually a function of r as well as s and ϕ_i, we shall replace $I_i(s,\phi_i,r)$ by $I_i(s,\phi_i)$ and often use $I_i(s)$ or $I_i(\phi_i)$ when the context makes it clear which parameter is meant.

In general $I_i \equiv I_i' + iI_i''$, which is either a normalized dielectric constant or a normalized impedance, will have a negative imaginary part for most measurements on liquid or solid C or D systems. Let I_i^* be the complex conjugate of I_i. We shall be interested in the frequency response of I_i^* for various ϕ_i and r values and of other normalized immittances in the D and C cases. In our present situation we must apparently deal with eight quantities and their relations, since the four basic immittance functions may be subscripted with either a C or a D. But because we need consider only I_i and its related normalized immittance functions, we need to use only four general functions to represent the full normalized M, Z, Y, and ϵ response of *both* the C and D systems. Table II shows the correspondences which follow when properly normalized functions are defined and introduced. In addition to the general I_i function, we have introduced three others, simply related to I_i, which like I_i may be used to represent normalized C- or D-system response. The definitions of these new general functions follow from the Table I relations, with μ redefined for simplicity as (is). Then for a fixed value of ϕ_i,

TABLE II. Relations between normalized immittance quantities for conductive and dielectric systems and the normalized quantities L_{iM}, I_i, S_{iM}, and T_{iM}.

Conductive system		General		Dielectric system
M_{CNM}	$\leftrightarrow$	L_{iM}	$\leftrightarrow$	Y_{DNM}
Z_{CN}	$\leftrightarrow$	I_i	$\leftrightarrow$	κ_D
Y_{CNM}	$\leftrightarrow$	S_{iM}	$\leftrightarrow$	M_{DNM}
κ_{CM}	$\leftrightarrow$	T_{iM}	$\leftrightarrow$	Z_{DM}

$$L_i \equiv isI_i, \tag{33}$$

$$L_{iM} \equiv L_i / L'_{i\infty}; \tag{34}$$

$$S_i \equiv I_i^{-1}, \tag{35}$$

$$S_{iM} \equiv S_i / S'_{i\infty}; \tag{36}$$

and

$$T_i \equiv L_i^{-1}, \tag{37}$$

$$T_{iM} \equiv L_{iM}^{-1}. \tag{38}$$

We have already normalized $I_i(s)$ so $I_i(0) = 1$. Therefore, $S_i(0)$ also equals unity. But what about $L'_i(\infty) \equiv L'_{i\infty}$ and $S'_{i\infty}$? We shall use the subscript "M" to denote quantities whose real parts have been normalized to unity at $s \to \infty$. Thus $Y_{DNM} \equiv Y_{DN}/Y_{DN\infty} \equiv L_{DM}$. The general quantity $L_{i\infty} = L'_{i\infty}$ is thus given by Eq. (24) for $Y_{DN\infty}$ with ϕ_D changed to ϕ_i.

We also need an expression for $S'_{i\infty}$. For $sW \gg 1$, Eq. (32) leads to

$$I_i \to [\phi_i/(r^{\phi_i} - 1)]\{s^{-2}[(r^{\phi_i - 2} - 1)/(\phi_i - 2)] - is^{-1}[(r^{\phi_i - 1} - 1)/(\phi_i - 1)]\}. \tag{39}$$

In this limit I'_i decreases with increasing s much faster than does I''_i. Therefore,

$$S_i = (I'_i - iI''_i)/(I'^2_i + I''^2_i) \to I'_i/I''^2_i - i(I''_i)^{-1}. \tag{40}$$

In the limit,

$$S'_{i\infty} = [(r^{\phi_i} - 1)/\phi_i][(r^{\phi_i - 2} - 1)/(\phi_i - 2)] \times [(\phi_i - 1)/(r^{\phi_i - 1} - 1)]^2. \tag{41}$$

It follows that $S'_{i\infty}(1 - n) = S'_{i\infty}(1 + n)$; $S'_{i\infty}(\phi_i)$ reaches a maximum value ≥ 1 at $\phi_i = 1$; and $S'_{i\infty}(\infty) = 1$. The quantity T_{iM}, which may be interpreted as either $\kappa_{CM} \equiv \kappa_C L_{C\infty}$ or $Z_{DM} = Z_D L_{D\infty}$, is here normalized to unity at $s \to \infty$. It should perhaps be normalized to unity at $s = 0$ but cannot be because $T_{iM}(0) = \infty$, reflecting the effects of a nonzero κ_D and a nonzero Z_C at $s = 0$. We have included the function T_{iM} primarily for completeness since it is generally less interesting than the other three functions.

D. Power-law exponents and possible temperature dependence

All the relationships shown in Table II arise because I_C and I_D may be written in a common form. They hold whenever this is the case, independent of whether or not a DRT or DAE is involved; they are thus completely general and do not depend on the particular DAE choice of Eq. (5). Table II shows that to investigate the response of such associated D and C systems one need only calculate I_i, and the L_i and S_i functions which follow from it, in order to obtain the response of all eight related normalized immittance functions. This will be done in the next section. Because of our normalization choices, all I_i, L_{iM}, and S_{iM} results will have real parts which fall between 0 and 1. All Table II relations also hold without $s \to \infty$ normalization.

We have defined both ϕ_D and ϕ_C, related by $\phi_C = \phi_D + (\alpha - \beta)/(\alpha + \beta)$. It turns out in the next section that there are finite-length regions in the L_{iM} and S_i plots which closely approximate $(is)^{n_i}$ behavior when n_i is not too far from 0.5, response characteristic of a CPE. The corresponding DAE factor n_i is then given by

$$n_D \simeq \psi_D \equiv 1 - \phi_D = (\alpha + \lambda)/(\alpha + \beta), \tag{42}$$

and

$$n_C \simeq \phi_C = (\alpha - \lambda)/(\alpha + \beta). \tag{43}$$

Although ψ_D and ϕ_C are not restricted by the present analysis to the range between 0 and 1, as we shall see later when n_i begins to depart appreciably from 0.5, DAE $(is)^{n_i}$ response is no longer always found, although individual real and imaginary parts of a given response function may still show power-law frequency dependence, but with somewhat different exponent values.

One important virtue of the present DAE analysis, as opposed to a DRT model based only on Eq. (14), is that it yields information on the form of possible temperature dependence of the n_i's. Although several somewhat microscopic theories, based on hopping conduction, free volume, percolation, etc., have been derived which lead to $(is)^{n_i}$ dependence over a limited frequency range, they usually yield no predictions of n_i temperature dependence and never lead to such dependence involving basic microscopic model parameters. In the present DAE situation, it is physically reasonable to take the η of Eq. (4) temperature independent[9,10]; then $\lambda = kT\eta$, directly proportional to absolute temperature.

The possible dependence of α and β on T may be more complicated. If only E is distributed, α and β are temperature independent if ordinary thermal activation behavior is present. Then

$$\psi_D = A_1 + B_1 T \tag{44}$$

and

$$\phi_C = A_1 - B_1 T, \tag{45}$$

where $A_1 \equiv \alpha/(\alpha + \beta)$ and $B_1 \equiv k\eta/(\alpha + \beta)$. When $\alpha > 0$ and $\beta = 0$, ψ_D increases linearly from unity at $T = 0$ to larger values for nonzero T, and ϕ_C decreases from unity in the same way. It is, in fact, very often found experimentally that n_i decreases with increasing T for conductive systems.[19] Further, response of the form $n_D \cong B_1 T \simeq \psi_D$ has been found experimentally for a dielectric system.[10] An n_i exponent decreasing with increasing temperature is usually associated with a C system and the opposite behavior with a D system.

Now consider the more complicated but not unlikely case where the entropy of activation ΔS and the activation enthalpy ΔH, here E, are both distributed and are linearly

related,[8–10] so $\Delta H = T_0 \Delta S$. The temperature T_0 is usually appreciably above any experimental temperature possible without phase or structure change. Then α and β are each proportional to $[1 - (T/T_0)]$, where T_0 may possibly be different for each one. It follows that A_1 may be temperature dependent (if the T_0's are different), and B_1 will be. Experimental and theoretical results of this kind have been given previously.[9,10] Finally, the material considered may exhibit a glasslike transition and thus satisfy a type of William–Landel–Ferry (WLF) equation,[8] and may also involve a linear relation between ΔS and ΔH as well. In this most complicated case, one must introduce another temperature constant T_∞, the Vogel temperature, usually 10–100° absolute below the glass transition temperature. Then for the range $T_\infty < T < T_0$, both α and β may be of the form

$$\chi_j = \chi_{0j}\left(\frac{1}{T} - \frac{1}{T_{0j}}\right)\left(\frac{T}{1 - (T_{\infty j}/T)}\right), \tag{46}$$

where $\chi_1 \equiv \alpha, \chi_2 \equiv \beta$, and $\chi_{01} \equiv \alpha_0, \chi_{02} \equiv \beta_0$. Here α_0 and β_0 are the original temperature-independent α and β which would apply if $T_0 \to \infty$ and $T_\infty \to 0$ (no relation between ΔH and ΔS and no glass transition). We shall not attempt to show curves of the possible temperature dependence of ψ_D and ϕ_C given by Eqs. (44) and (45) since in the worst case they involve the seven parameters T_{0j}, $T_{\infty j}, \chi_{0j}$, and η. In principle, values of these parameters may be estimated using experimental n_i values and nonlinear least-squares fitting. In most cases of interest, however, $T_{\infty j}$ will be zero and $T_{01} = T_{02} = T_0$; then only T_0, α_0, β_0, and η will need to be determined. A final simplification occurs in cases where the capacitance is not thermally activated and $\beta_0 = 0$.

It is important to note that since $-\infty < \phi_i < \infty$, the quantity ϕ_i is not limited to the 0–1 range of the usual n_i exponents, and so ϕ_i can depend directly on T in ways impossible for these exponents. In future work, approximate relations will be discussed between the n_i's associated with various conventional fitting expressions, such as that of Davidson and Cole, and the DAE ϕ_i parameter. Such relations can be used to interpret directly measured n_i temperature dependence for such empirical models in terms of the temperature dependence of the physically realistic DAE model.

IV. DISCUSSION OF RESULTS

A. Two- and three-dimensional response for I_i^* and L_{iM}

In the next sections we shall present and discuss results for the response functions I_i^*, L_{iM}, and S_i obtained using the exact expressions of Appendix B. Both two-dimensional complex plane plots with frequency as an implicit variable and three-dimensional plots with perspective, which include frequency variation explicitly,[20] will be presented. We shall begin by considering I_i^* and L_{iM} 2D plots. For such plots we find that a symmetry relation holds and reduces the need to show both types of results for all values of ϕ_i of interest.

The relation, which follows from the form of Eq. (32), is

$$L_{iM}(q, \psi_i) = I_I^*(s, \phi_i), \tag{47}$$

with

$$\psi_i + \phi_i \equiv 1 \tag{48}$$

and

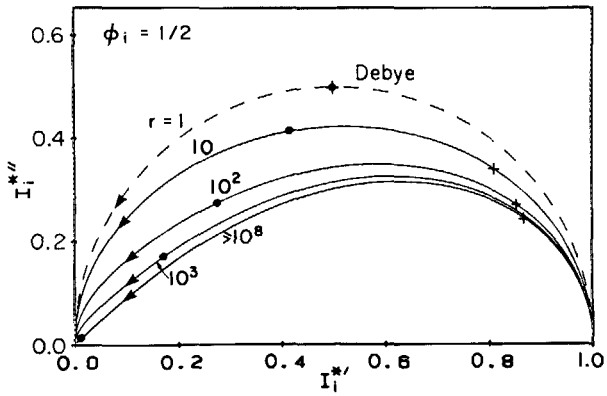

FIG. 1. Complex plane plot of I_i^* for $\phi_i = 0.5$ and a variety of r values. Solid circle: points at which $s = s_e \equiv r^{-1/2}$; cross: points where $s = s_r \equiv r^{-1}$.

$$q \equiv (rs)^{-1}. \tag{49}$$

Because of these equations, 2D $I_i^*(\phi_i)$ curves may also be considered to be $L_{iM}(1 - \phi_i)$ curves with the frequency direction reversed. Therefore, we need not show separate 2D L_{iM} curves. Figures 1 and 2 show how the shapes of I_i^* plotted in the complex plane depend on r at constant ϕ_i and on ϕ_i at constant r. The dashed-line 2D curves shown here and later are for simple Debye response, that which follows in the present analysis when $r \to 1$ for any ϕ_i, or for $\phi_i \to \pm\infty$ for any r. They are included to show how $r > 1$ curves with finite ϕ_i values differ from single-time-constant response. The arrows show the direction of increasing frequency.

Equation (49) shows that there is a single frequency, $s = s_e \equiv r^{-1/2}$, at which $q = s$, the one frequency where $I_i^*(\phi_i)$ and $L_{iM}(1 - \phi_i)$ will have equal real and imaginary parts. Such equality occurs at different frequencies otherwise. To provide some indication of frequency dependence, we shall mark the s_e point on many of the 2D plots as a solid dot and shall also show the $s = s_r \equiv r^{-1}$ point with a cross symbol. Note that $s_r r = 1$ is equivalent to $\omega\tau_\infty = 1$. Thus below this frequency single-time-constant response dominates. We see from Fig. 1 that as r increases the shape of the curve has almost reached its $r \to \infty$ limiting value (here well represented by $r = 10^8$) by $r = 10^3$. But note that the s_e point will occur at lower and lower frequencies as r increases, even though the shape stabilizes. Thus, as already stated, as $r \to \infty$ and there is thus no finite maximum activation energy, all the response is forced to the $s \to 0$ frequency point, leaving nothing measurable. The figure also shows that when $\phi_i = 0.5$ all the s_e solid-dot points lie on the specific 45° line for which $I_i^{*\prime} = I_i^{*\prime\prime}$.

Figure 2 shows more I_i^* 2D curves for other ϕ_i values in the large r region ($r = 10^8$). It is found that for $\phi_i = -0.5$, where the basic integral, Eq. (32), converges when $r \to \infty$, not only does the shape stabilize but the frequency distribution along the curve stabilizes as well. Thus for this single curve (or any others with $\phi_i < 0$) it is appropriate to show absolute normalized frequencies as well as s_e and s_r. The result for $\phi_i = 0$ is a transitional one. As $r \to \infty$, the value of $(I_i^{*\prime\prime})_{\max}$ decreases as $[\ln(r)]^{-1}$, although the s_e point remains in the center. Thus as r increases the shape never entirely stabilizes but the flat portion becomes longer and its height smaller.

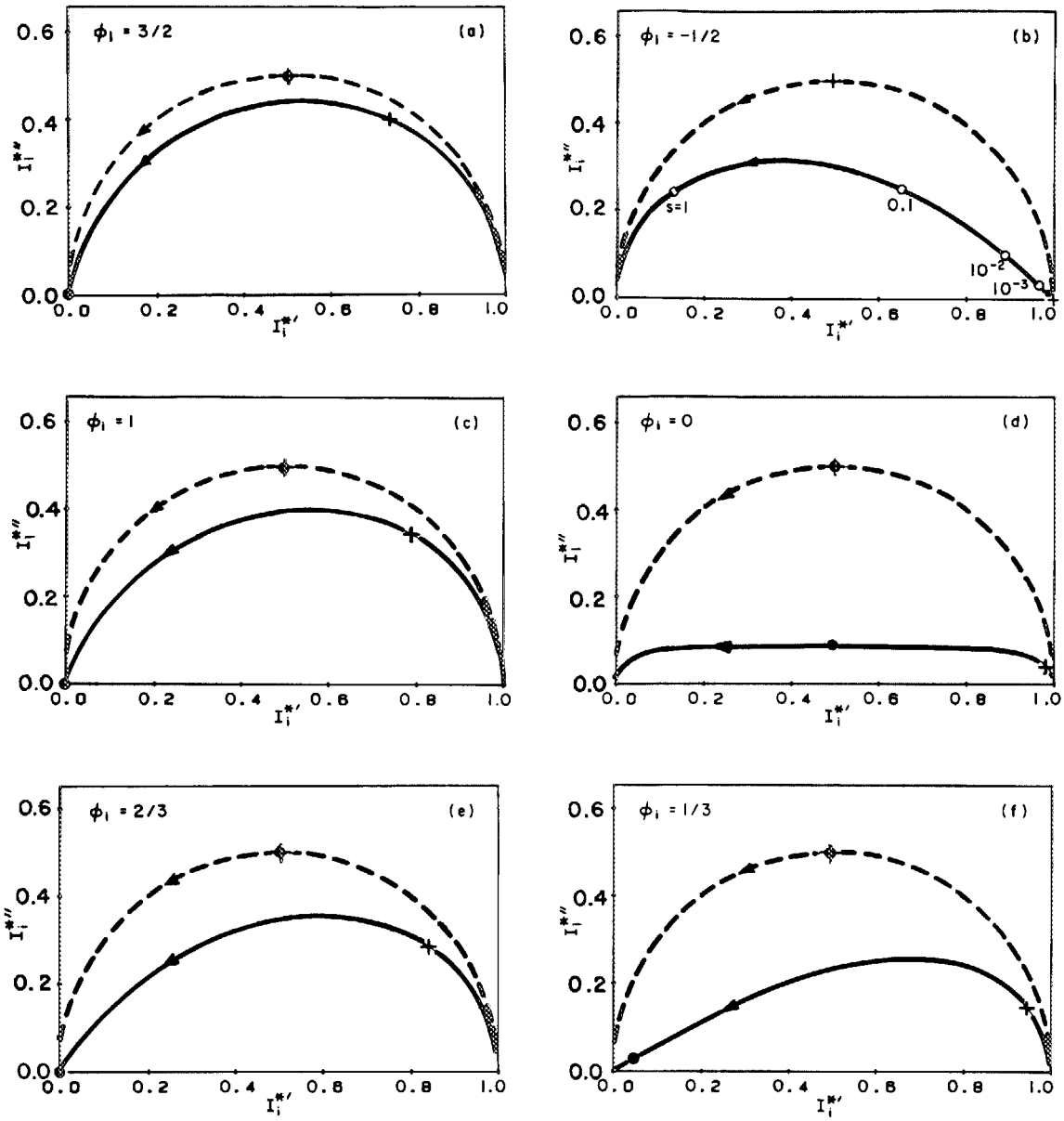

FIG. 2. Complex plane I_i^* plots for $r = 10^8$ (solid lines) and a variety of ϕ_i values. Dashed-line curves for $r = 1$.

Again in the $r \to \infty$ limit there will be no measurable response. For all $\phi_i > 0$ values, the shape stabilizes at large r and the $s = s_e$ point remains at the same position. Thus again all curves for $\phi_i > 0$ collapse into the frequency origin as $r \to \infty$. The angles which the straight-line parts of such curves as Figs. 2(b) and 2(f) make with the horizontal axis are approximately given by $(\phi_i \pi/2)$.

Let us now consider 3D perspective plots for $I_i^*(\phi_i)$ and $L_{iM}(\psi_i)$ response for different ϕ_i values, all with $r = 10^8$. Figure 3 shows such curves, where for each separate graph we have plotted two 3D curves (heavy lines) and their projections. The viewpoint is nearly the same for all these curves. The grouping used is such that curves satisfying the symmetry relations, Eqs. (47) and (48), are together. The dashed projection curves are for $I_i^*(\phi_i)$ and the solid ones for $L_{iM}(\psi_i)$. This grouping, of course, yields identical x-y and complex-plane projections, as shown. The point at which the two 3D curves cross is at $s = s_e$. The symmetry relations of Eqs. (47)–(49) ensure that the projection curves in the Im-log(s) plane are mirror images of each other around this crossover point. Because each 3D curve in Fig. 3(c) is separately symmetric about its center at $s = s_e$, the two mirror-image curves in the Im-log(s) plane degenerate to a single one for this case. Note that the $\phi_i = 0$ choice is the one which approximates as well as possible Garton's[2] original goal of finding conditions that lead to ϵ'' (here $I^{*\prime\prime}$) independent of frequency.

Although even 3D plots with perspective don't show the shapes of the complex plane projection curves perfectly (without using stereoscopic pairs), these shapes are shown exactly, along with other information, in Figs. 1 and 2. For all linear 3D plots shown, the zeros of the real and imaginary scales are at the origin and the scale unit is 0.1 (all curves normalized to unity at $s \to 0$ or $s \to \infty$). The unit of the log(s) scale is always 1 (factor of 10), and its origin is as stated on each plot.

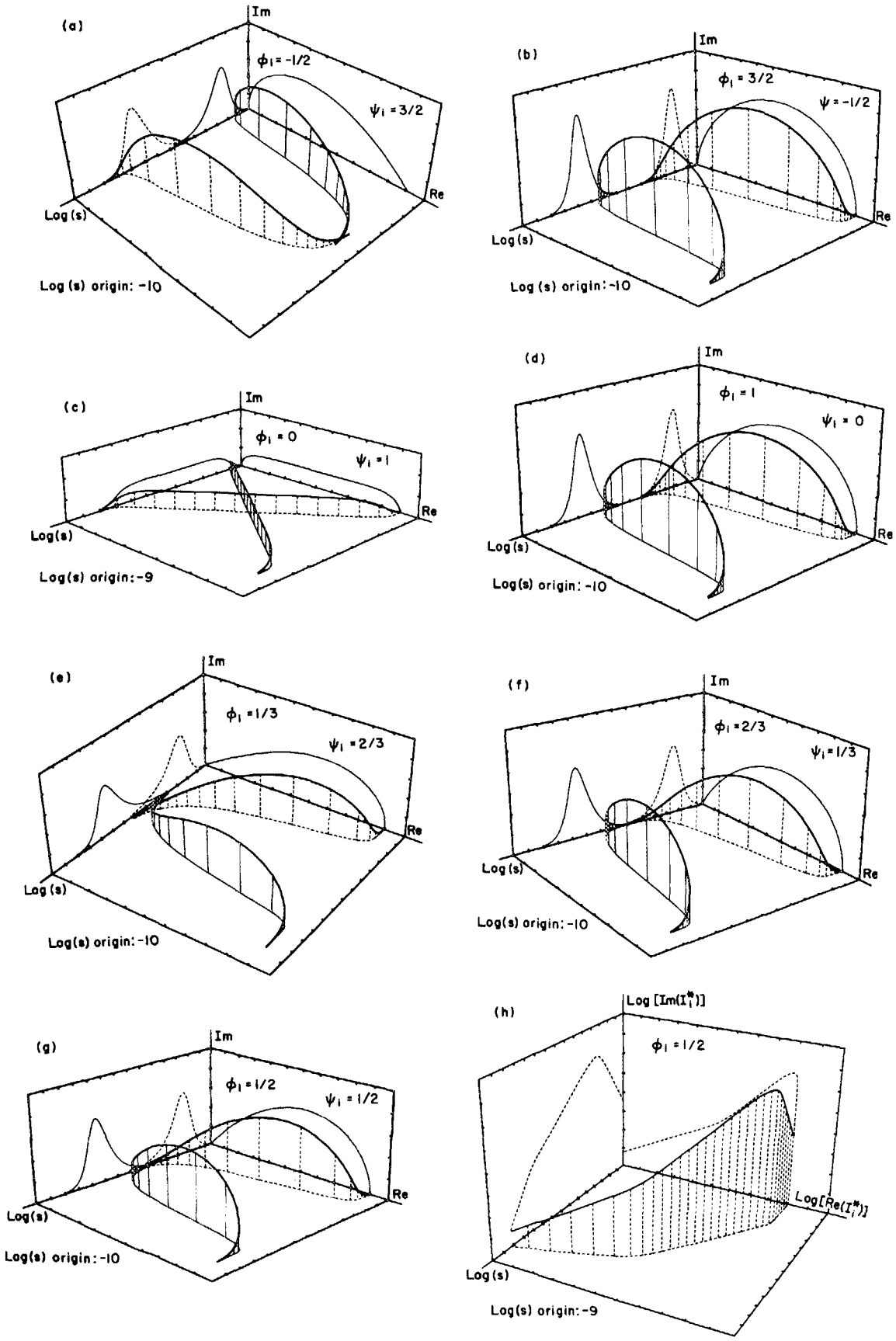

FIG. 3. Three-dimensional projection curves with perspective for $I_i^*(\phi_i)$ (2D projections shown dotted) and $L_{iM}(\psi_i)$ (2D projections shown solid) for $r = 10^8$ and a variety of $\phi_i = 1 - \psi_i$ values. Part (h) uses $\log_{10}$ rather than linear complex plane scales.

There are, of course, two disparate physical interpretations of the 3D curves in Fig. 3. If a D system is being considered, then $I_D(\phi_D) \equiv \kappa_D$ and $L_{DM}(\psi_D) \equiv Y_{DNM}$; thus one of the two curves represents the (normalized) complex dielectric constant with $\psi_D \equiv 1 - \phi_D$ and the other a (normalized) admittance for the same $\psi_D \equiv 1 - \phi_D$. But although the ψ_D's are the same, the curves do not represent the complex dielectric constant and admittance of the same material, except for the Fig. 3(g) results. Since $Y_{DN} \equiv L_D = isI_D \equiv is\kappa_D$, if say $\kappa_D'' \propto s^{\psi_D - 1}$ in a certain frequency range, then Y_{DN} will be proportional to s^{ψ_D} in this range. The definitions of Eqs. (33)–(38) show that curves at various levels which are all associated with the same material involve the same ϕ_D or ψ_D. Thus the $I_i(-1/2)$ curve of Fig. 3(a) is associated with the $L_{iM}(-1/2)$ curve of Fig. 3(b). Alternatively, for a C system the results of Table II show that the two 3D curves of say Fig. 3(a) may be interpreted as $I_C(-1/2) = Z_{CN}(-1/2)$ and $L_{CM}(3/2) = M_{CNM}(3/2)$; the $Z_{CN}(-1/2)$ curve is associated with $M_{CNM}(-1/2)$ and the $Z_{CN}(3/2)$ curve with $M_{CNM}(3/2)$.

The log-log 3D plot of Fig. 3(h) is included to demonstrate several important points. First for this $r = 10^8$ log-log $I_i^*(1/2)$ curve and its projections, we see that there are three separate straight-line regions. To a good approximation we find for the log(Im) – log(Re) plane that there is a unity slope region extending over more than three decades of $I_i^{*\prime}$ and $I_i^{*\prime\prime}$ variation in the mid-frequency range, a rapid dropoff at low frequencies, and a high-frequency region of slope 0.5. It can be readily shown from the integral representation, Eq. (32), that as $s \to 0$, $I_i^{*\prime\prime}$ becomes proportional to s and $(1 - I_i^{*\prime}) \propto s^2$ for any ϕ_i. Similarly, for $s \to \infty$, $I_i^{*\prime\prime} \propto s^{-1}$ and $I_i^{*\prime} \propto s^{-2}$, independent of ϕ_i. The slopes in Fig. 3(h) are consistent with these results. Note especially that $\mathrm{Im}(I_i^*)$ and $\mathrm{Re}(I_i^*)$ show CPE-type $s^{-\phi_i} = s^{-1/2}$ behavior over more than seven decades of frequency, with the actual number of decades of such response proportional to $\log(r)$. This long straight-line response corresponds, however, to only about three decades of straight-line variation in the corresponding complex plane plot. Of particular importance is the $s \to \infty$ response. For a C system it is consistent with that of a resistor and capacitor in parallel and for a D system the high-frequency response is the same as that of a resistor and capacitor in series, proper results for these two kinds of systems. Full limiting equivalent circuits will be discussed later. It is noteworthy that the CPE and several other models for D or C small-signal frequency response (see later discussion) do not show such physically plausible limiting behavior but continue to exhibit $s^{-\phi_i}$ response (at the I_i^* level) for arbitrarily high frequencies.

B. Comparison with response of other distributed elements

A great deal of C- and D-system data accumulated over many years for many different materials lead to complex plane and 3D frequency response results qualitatively and often quantitatively similar to the results of Figs. 1–3 for the present DAE system.[4,5,14,16,18,21–29] Results are most often found which yield a region of CPE-like, straight-line complex-plane behavior of the kind seen in Figs. 3(e), 3(f), and 3(g) for $\phi_i = 1/3$, $1/2$, and $2/3$. On the other hand, the reverse sort of behavior, where the straight line appears at the low-frequency side, as in Fig. 3(a), is also sometimes found.[29] Both types of behavior also appear for C-system Y plots for a material having both positive and negative charges mobile with different mobilities.[30]

One reason the present DAE model can lead to 2D and 3D curves of the type exhibited by a wide range of C- and D-system data is that its predictions, when ϕ_i and r are both disposable, are similar to those of several other models (DRT ones or otherwise) which have commonly been used to fit such data quite well [though only a small amount of fitting of both real and imaginary parts of data simultaneously by complex nonlinear least squares[25,26] (CNLS) has been carried out thus far[23–26,28]]. These distributed-element functions will be given in general I_i form so they may be applied to either C and D systems. The ones of most interest are

$$I_{ia} = (is)^{-\psi_i}, \tag{50}$$

$$I_{ib} = [1 + (is)^{\psi_i}]^{-1}, \tag{51}$$

$$I_{ic} = (is)^{-\psi_i} \tanh(is)^{\psi_i}, \tag{52}$$

$$I_{id} = (1 + is)^{-\psi_i}, \tag{53}$$

and

$$I_{ie} = \text{Williams–Watts response.} \tag{54}$$

In all these results s is an arbitrary normalized frequency, not necessarily the specific s of the present DAE model. Although there need not be any relation between the ψ_D and ψ_C of these equations, in the few instances where the same form has been applied for both D and C systems it has been customary to take $\psi_D = 1 - \psi_C$. This makes frequency-dependence exponents the same for Y_{DN} and Y_{CN} [see also Eqs. (42) and (43)]. All the expressions above hold for $0 \leqslant \psi_i < 1$, and all but that of Eq. (52) also hold for $\psi_i \leqslant 1$.

The first of the above functions is the CPE. Because it cannot be normalized at $s = 0$, when it appears alone it cannot be interpreted as a normalized I_i of the form of Eq. (22) or Eq. (31). For convenience, we nevertheless write it as an I_i with the understanding that for this case only I_i is just a dimensionless form of a complex dielectric constant or impedance. The second formula is just that for the Cole–Cole[4] response function when interpreted for a D system, and it is what may be called the ZARC function for a C system.[31,32] Further, for a C system it may be represented by a CPE and resistor in parallel and for a D system as a CPE and capacitor in series. We shall designate it here as the ZC model. It leads (for $0 < \psi_i < 1$) to complex plane ϵ or Z plots which are arcs of a circle whose center is displaced below the real axis. Although such symmetrical curves are in fact often found experimentally for both D and C system response over a limited frequency range, it is perhaps more common to find unsymmetrical response of the present DAE type, response which yields an approach to the real axis with a 90° slope at sufficiently high or low frequencies. Such response implies the presence of a shortest and a longest time constant for the system, necessary results for any real system.

The third function is, for $\psi_i = 0.5$, just finite-length Warburg response, associated with one-dimensional uniform diffusion in a finite space.[33] Here we have generalized such response by introducing an arbitrary $\psi_i (0 \leqslant \psi_i < 1)$ in order to allow comparison with the other functions and, perhaps, approximately represent diffusion in an inhomogeneous region.[34] The generalized response function will be denoted the GFW. For I_{Cc} the function is a normalized impedance whose analog for $\psi_C = 0.5$ is a short-circuited uniform transmission line, while I_{Dc} for $\psi_D = 0.5$ is a normalized complex dielectric constant function whose analog response is that of an open-circuited transmission line.[33,35]

The function I_{Dd} was originally introduced by Davidson and Cole[5] (DC) and yields[5,18] asymmetric response rather like the present DAE except for $s \to \infty$. The corresponding I_{Cd} function has not been introduced or used heretofore at the impedance level. Williams–Watts (WW) frequency response[36–38] is associated with transient response of the form $\exp(-t/\tau_0)^{\psi_i}$ and is thus often termed fractional exponential response. There are closed-form expressions for I_{ie} available for only a few specific values of ψ_i but series expressions for I_{ie} have been given.[39] Williams–Watts response was originally introduced for D systems and has been primarily applied for fitting small-signal ac dielectric data. It has also been introduced through its approximate DRT at the M level (same results as for a DRT at the Z level), however, for conductive systems.[40] Kenkel has shown that D-system WW frequency response can be reasonably well approximated by a circuit consisting of a CPE in parallel with a resistor and all in series with an ideal capacitor.[41] One difference between all the functions mentioned is that if they are normalized to unity at $s = 0$, then they all exhibit somewhat different maximum values of $I_i^{*\prime\prime}$ (maximum height in a 2D complex plane plot). These heights for $\psi_i = \phi_i = 0.5$ are found to be ZC: 0.207; WW: 0.274; present DAE: 0.315; DC: 0.354; and generalized finite-length Warburg (GFW): 0.417. The result for the DAE is that for $r \geqslant 10^8$; a larger maximum value appears for smaller r.

The GFW, DC, WW, and DAE expressions all lead to asymmetric curves in the complex plane when ψ_i or ϕ_i are between 0 and 1. It turns out that although the curves have different normalized heights when all the ψ_i and ϕ_i's are equal they may nevertheless be made to fit each other reasonably well without additional circuit elements, provided the exponents are not very small, by taking the exponents unequal and adjusting the heights. Thus, for example, CNLS fitting of $\psi_i = 0.5$ DC "data" with the DAE, or *vice versa*, leads to quite close fits over a wide frequency range, often within the accuracy of typical experimental data. This possibility of fitting one model by another or by more than one will be examined in detail elsewhere.

C. S_i response

Thus far we have not shown any plots of S_i or S_{iM}. We find that the quantity S_i, which is unity at $s = 0$, is especially useful in helping distinguish between models, particularly for the low-frequency region. But S_i'', which represents either Y_{CN}'' or M_{DN}'', is unlimited in magnitude as s increases. It is therefore not possible to show complete 2D curves graphically, and we shall use log-transformed as well as linear plots to cover a wide frequency range. Figure 4(a) shows the low frequency end of 3D S_i response for $\phi_i = 1/3$ and $r = 10^8$. Here the common x and y unit is 1.9. The complex plane curve shows the characteristic angle with the real axis of $(\phi_i \pi/2) \simeq 30°$. Figure 4(b) is a log plot covering much wider frequency and magnitude ranges. Its x and y axis origins are at 0 and -2, respectively. Like Fig. 3(h) it exhibits three straight-line regions for the 3D curve and its projections. Note especially the final rise where S_i' has reached its final value of about 371 and S_i'' is increasing proportional to s. For the C-system choice it is thus exhibiting response associated with a constant high-frequency-limiting capacitance.

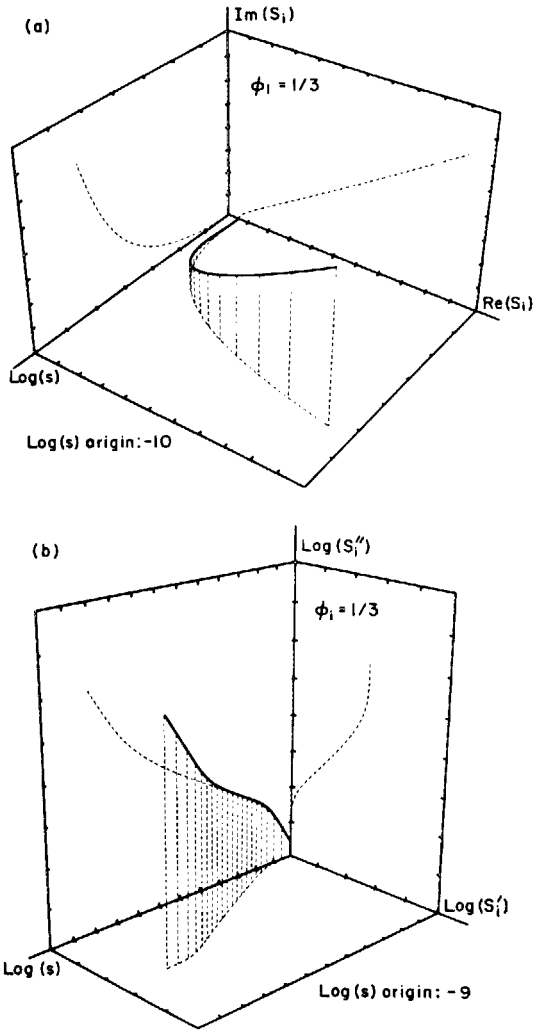

FIG. 4. (a) Three-dimensional curve and projections for S_i with $\phi_i = 1/3$ and $r = 10^8$. (b) Log-transformed 3D curve and projections for the same conditions as in (a).

It turns out that much significant detail and discrimination can be achieved with 2D S_i plots, linear and log. Figure 5(a) shows low-frequency linear 2D S_i curves for $\phi_i = 0.5$ and various r values (solid lines). In addition, the corresponding Debye curve is shown dash-dotted, the CPE dashed, and the ZC as a dash, dot, dot line. Here $\psi_i = 0.5$ for the CPE and ZC models. This plot shows very clearly indeed the differences in the low-frequency behavior of the various models. The DAE yields a Debye response for $r = 1$ and approaches a limiting curve falling between the CPE and the

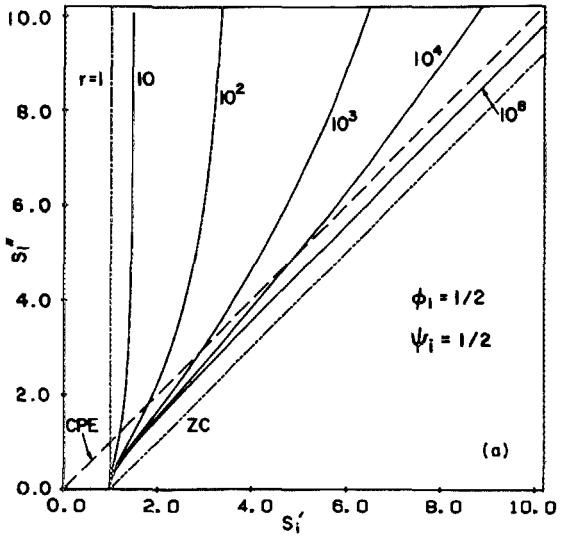

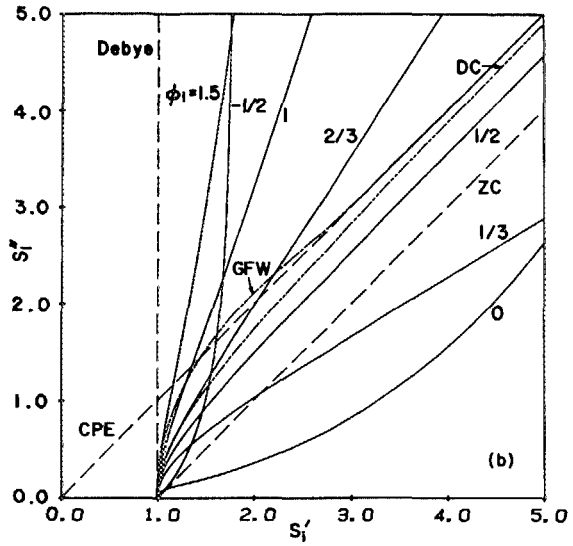

FIG. 5. Complex plane plots of S_i for the low-frequency region near the $S_i'(0) = 1$ origin. The curves for CPE, ZC, DC, and GFW distributed-element response are all for $\phi_i = 0.5$. In (a) the DAE curves are all for $\phi_i = 0.5$ and r is variable; in (b) $r = 10^8$ and ϕ_i is variable.

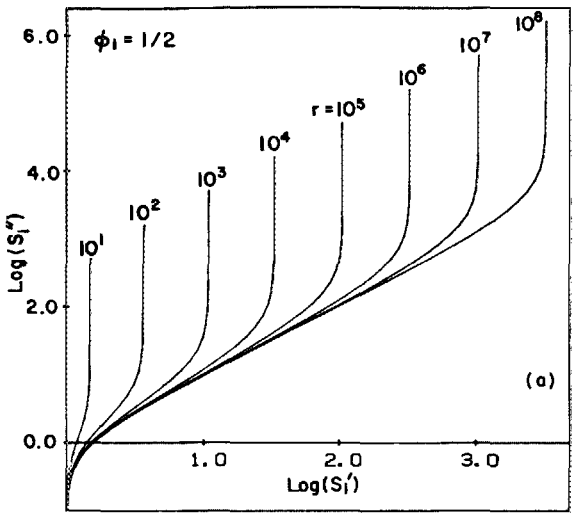

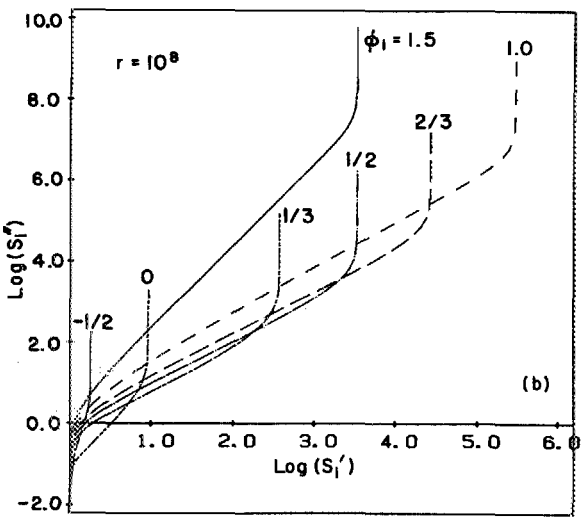

FIG. 6. Log-transformed complex plane plot of S_i. (a) $\phi_i = 0.5$, r variable; (b) $r = 10^8$, ϕ_i variable.

ZC as r increases indefinitely. Note that neither the CPE nor the ZC approaches the real axis at 90° for $s \to 0$ as the other curves do. Figure 5(b) is also a linear 2D S_i plot with several DAE curves, all for $r = 10^8$ but with different ϕ_i's, and in addition, Debye, GFW, CPE, DC, and ZC response curves are also included. For the last four curves $\psi_i = 0.5$ again. Note the characteristic overshoot of the GFW curve and the odd behavior of the $\phi_i = -0.5$ curve. If actual frequency response data can be plotted in the present way for sufficient low frequencies to show the final approach to $s_i'(0)$ (here unity), the detailed shape near the origin should greatly help in identifying the most appropriate model to represent the data.

Figures 6(a) and (b) present log-transformed DAE response only. Figure 6(a) is for $\phi_i = 0.5$ and various r's. Note that as r increases a longer and longer region with approximately unity log-log slope occurs. Figure 6(b) is for $r = 10^8$ and various ϕ_i's. Clearly the slopes of the inclined straight-line parts of the curves remain near unity for $0 < \phi_i < 1$; there is no appreciable intermediate-frequency straight-line region for $\phi_i = -0.5$; and the $\phi_i = 0$ and 1.5 curves show regions with a slope of two.

D. Slope and exponent results

The matter of linear and log slope factors requires somewhat more discussion because log slopes (power law exponents) are always calculated when small-signal frequency response data yield straight-line regions and because there are various slopes of interest which can be defined for response such as that of the present DAE system. Let us continue to use the symbol "n" to represent a frequency response power-law exponent or semilog-plot slope, particularly at the S_i level. Thus Eq. (50) for the CPE leads to $S_{iCPE} = (is)^{\psi_i}$, and we may set $n_{iCPE} = \psi_{iCPE}$. But such a simple relationship does not hold exactly for the DAE, as we shall see below. Second, let us use the symbol "m" to represent the slope of a straight-line region in the ordinary linear complex plane plot. For the linear region then $m \equiv \mathrm{Im}/\mathrm{Re}$. Let the associated angle in the complex plane be denoted by ζ. Then $m \equiv \tan(\zeta)$, and from

TABLE III. Log and linear slopes derived from straight-line response regions of log (S_i') and log (S_i'') plots for $r = 10^8$.

ϕ_i	n_R	n_I	p	ζ (deg.)
1/3	0.345	0.375	1.09	31.6
1/2	0.496	0.512	1.03	45.3
2/3	0.645	0.663	1.03	58.9
1	0.811	0.909	1.12	76.2
3/2	0.497	1	2.01	85.7

the $S_{i\,\mathrm{CPE}}$ expression one finds $m = S''_{i\mathrm{CPE}}/S'_{i\mathrm{CPE}} = \tan(\zeta) = \tan(\psi_{i\mathrm{CPE}}\pi/2)$.

Now the DAE does not always yield the linear relation between Im and Re which applies for the CPE. Instead one finds straight-line regions in log(Im), log(Re) log-transformed complex plane plots which can be well represented by $\mathrm{Im} = A_2(\mathrm{Re})^p$. For the CPE one finds that $p = 1$ and $A_2 = \tan(\zeta) = m$, but these results do not apply exactly for the DAE. Table III lists n and p values determined from least-squares fitting of frequency response results limited to the straight-line regions appearing in Fig. 6(b) for various ϕ_i values and $r = 10^8$. The exponents n_R and n_I are defined by the relations $S_i' = A_3(s)^{n_R}$ and $S_i'' = A_4(s)^{n_I}$. From these relations it follows that $p = n_I/n_R$. We see that although n_R and n_I values approximate ϕ_i ones, n_R,n_I, and ϕ_i are clearly different quantities except when r_1 becomes very large; then these quantities closely approach one another for $0 < \phi_i < 1$. Although the calculation of m values is only appropriate when $p = 1$, we have found that for frequency values nearer $s = 0$ than those which led to the n_R,n_I, and p values shown, there are regions which yield good straight lines on a linear plot, as in Fig. 5(b). The values shown for $\zeta = \tan^{-1}(m)$ are calculated for these nearly linear regions, but it should be cautioned that m values tend to increase somewhat as regions further from the origin are sampled, with such increase associated with the $p > 1$ values present for larger s regions. Particularly for the larger ϕ_i values as ϕ_i increases, the adequacy of a linear fit decreases. At $\phi_i = 3/2$ a square-law curve is being approximated by a linear one but because the slope is so great in the linear plot, a reasonably good straight line can nevertheless be fitted over a limited range. The range used for the $\phi_i = 3/2$ ζ value shown was $10^{-7} \leqslant s \leqslant 10^{-6}$; if one uses $10^{-5} \leqslant s \leqslant 10^{-4}$ instead, one finds $\zeta \sim 89°$.

As $\phi_i \to 0$, the DAE and CPE models yield different but somewhat similar results. Consider C-system response. For $\phi_C = 0$ the CPE Z_{CN} equals unity, a pure resistor with no imaginary part or frequency dependence. As Figs. 2(d) and 3(c) show, $\phi_C = 0$ DAE response for $r = 10^8$ can lead to a wide frequency range where $|Z''_{CN}|$ is very small and constant, but over this range Z'_{CN} varies as $[\log(1/s)]/8$ from about 0.8 to 0.2. Although DAE response in the intermediate frequency range is somewhat like that of the CPE for $0 < \phi_i \lesssim 0.6$, when $\phi_i = 1$ the CPE leads to pure capacitance response for both $i = D$ and $i = C$. On the other hand, as we have seen, e.g., Fig. 6, S_C DAE response involves a frequency-dependent conductance and frequency-dependent capacitor, which, at high frequencies, reduce to a frequency-independent conductance and capacitance. But for $\phi_i > 2$, the conductance rapidly approaches no variation at all. For example, $S'_{i0} = 1$ and $S'_{i\infty} \cong 11/5$, 4/3, and 16/15 for $\phi_i = 2$, 3, and 5, respectively, for $r \geqslant 10^8$. For large ϕ_i, S_i may thus be well represented over the entire frequency range of interest by its $s \to \infty$ limiting response, described by the simple equivalent circuits discussed below. In an approximate sense, we can take $\psi_{i\mathrm{CPE}}$ and the ϕ_i for the DAE nearly the same for $0 \leqslant \phi_i \lesssim 0.6$, but above $0.6\,\phi_i$ is stretched so that response approximately like that of the CPE with $\psi_{i\mathrm{CPE}} = 1$ only occurs when $\phi_i \gtrsim 3$.

Finally, it is of interest to compare approximate frequency dependence exponents n for all the real and imaginary parts of the four general functions for a reasonably wide range of ϕ_i values. Table IV presents such results for very large r. We see from these results and those in Table III that for ϕ_i not too far from 0.5, S_i and L_i involve $n \cong \phi_i$ exponents but the situation is more complex for ϕ_i values further removed from 0.5. The line of results for $\phi_i \geqslant 3$ is the same as that obtained for simple Debye response. The symmetry, with sign changes, apparent in this table, e.g., compare appropriate $\phi_i = -1/2$ and $\phi_i = 3/2$ results, is, of course, associated with the symmetry relations of Eqs. (47)–(49).

E. Limiting equivalent circuits for D and C systems and an approach to data analysis

Next it is useful to consider the equivalent circuits which represent ideal D- and C-system response as $s \to 0$ and $s \to \infty$. From Eqs. (22), (23), and $Y_D = i\omega C_c \epsilon_D$, one may write

$$Y_D = i\omega[(C_0 - C_\infty)J_D + C_\infty]. \tag{55}$$

Similarly, Eq. (31) leads to

$$Z_C = (R_0 - R_\infty)J_C + R_\infty. \tag{56}$$

We shall use the minimum τ, $\tau_0 \equiv s/\omega$, the $\mathscr{E} = \mathscr{E}_0$ value of τ; see Eqs. (8) and (17). Now one finds that expansions of Eq. (32) in the $s \to 0$ and $s \to \infty$ limits lead to expressions for I_C and I_D in these limits which, together with Eqs. (55) and (56), yield the equivalent circuits of Fig. 7 and the specific limiting

TABLE IV. Frequency dependence exponents. Approximate values of n for intermediate-frequency-region response of the form s^n.

ϕ_i	I_i'	I_i''	S_i'	S_i''	L_i'	L_i''	T_i'	T_i''	n_C	n_D
−0.5	0	0.5	0	0.5	1.5	1	−0.5	−1	−0.5	1.5
0.5	−0.5	−0.5	0.5	0.5	0.5	0.5	−0.5	−0.5	0.5	0.5
1.5	−1.5	−1	0.5	1	0	−0.5	0	−0.5	1.5	−0.5
>3	−2	−1	0	1	0	−1	0	−1	>3	<−2

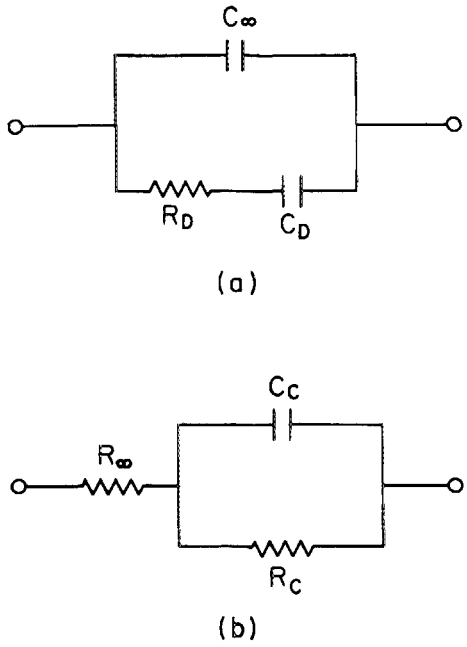

FIG. 7. Equivalent circuits for full dielectric (a) and conductive (b) system response for the $\omega \to 0$ and $\omega \to \infty$ limits. Parameter expressions for these cases are given in Table V.

parameter values listed in Table V. Note that the same equivalent circuit is appropriate for a given system for both low and high frequencies, although circuit element values are different in these two limits. In Table V the various N's are defined by

$$N_j \equiv (\phi_i + j)/(r^{\phi_i + j} - 1). \tag{57}$$

Thus the $S'_{i\infty}$ quantity of Eq. (41) is just $(N^2_{-1}/(N_0 N_{-2})$. Since we are dealing with D and C systems having the same formal DAE's and DRT's, the low-frequency time constant τ_{i0} is the same for both systems, as is the high-frequency one, $\tau_{i\infty}$. Incidentally, the $s \to 0$ results hold well for $s \lesssim s_r$ and the $s \to \infty$ ones hold for $s \gtrsim 10$. For a real C system, the Fig. 7(b) circuit should be augmented by adding a C_∞ element in parallel with it. Such an element is always present because $\epsilon_\infty > 0$ for any system.

From Table V we may form the additional ratios

$$\tau_{i0}/\tau_{i\infty} = (N_0 N_{-1}/N_1 N_{-2}) \to r, \tag{58}$$

$$R_{C0}/R_{C\infty} = C_{D0}/C_{D\infty} = S'_{i\infty} \to \sqrt{r}/3, \tag{59}$$

$$R_{D0}/R_{D\infty} = C_{C0}/C_{C\infty} = N_0^2/(N_{-1} N_1) \to r^{3/2}/3, \tag{60}$$

TABLE V. Expressions for the $\omega \to 0$ and $\omega \to \infty$ limiting capacitances and resistances of Fig. 7 for associated dielectric and conductive systems.

$i = D$ or C	Dielectric system	Conductive system
R_{i0}	$[\tau_0/(C - C_\infty)](N_0/N_1)$	$(R_0 - R_\infty)$
C_{i0}	$(C_0 - C_\infty)$	$[\tau_0/(R_0 - R_\infty)](N_0/N_1)$
τ_{i0}	$\tau_0(N_0/N_1)$	$\tau_0(N_0/N_1)$
$R_{i\infty}$	$[\tau_0/(C_0 - C_\infty)](N_{-1}/N_0)$	$(R_0 - R_\infty)(N_0 N_{-2}/N^2_{-1})$
$C_{i\infty}$	$(C_0 - C_\infty)(N_0 N_{-2}/N^2_{-1})$	$[\tau_0/(R_0 - R_\infty)](N_{-1}/N_0)$
$\tau_{i\infty}$	$\tau_0(N_{-2}/N_{-1})$	$\tau_0(N_{-2}/N_{-1})$

where the arrows lead to the large-r limiting values appropriate for $\phi_i = 0.5$ only. For large r and $\phi_i > 1$, however, $R_{D0}/R_{D\infty}$, for example, goes to $\phi_i^2/[(\phi_i - 1)(\phi_i + 2)]$, which approaches unity as $\phi_i \to \infty$. As one would expect, $\tau_{i0}/\tau_{i\infty} \geq 1$.

Now fitting experimental small-signal D or C data to an equivalent circuit is most appropriately carried out using CNLS.[25] A CNLS fitting routine is available from the author which includes in the equivalent circuit the choice of various distributed element models, including that of the DAE, represented by Eq. (32). Any of these elements may be embedded in a full circuit involving other capacitative, inductive, and resistive elements. For a D-system DAE model, such fitting yields estimates of τ_0, r, ϕ_D, and C_{D0} while fitting with the DAE model appropriate for a C system, yields estimates of τ_0, r, ϕ_C, and R_{C0}.

Consider, as an example of possible fitting and analysis, the C-system parameter estimates in more detail. Suppose the results are obtained for a number of different temperatures and that the DAE model appears to fit the data well. Then the above four parameter estimates will be well determined, with small relative standard errors, at each temperature. But more can be learned from the temperature dependence of the estimates of $r \equiv \exp[\gamma(\mathscr{E}_\infty - \mathscr{E}_0)]$, $\tau_0 \equiv \tau_a \exp(\gamma_0)$, and $\phi_C \equiv (\alpha - kT\eta)/\gamma$, remembering that E_0, E_∞, τ_a, and η are all taken temperature independent.

Although much of the shape of say an I^*_C complex plane plot becomes independent of r for large r when $\phi_C \geq 0$, the high- and low-frequency-limiting responses and the size of Z_C responses are nevertheless dependent on r, as shown by the results of Table V and Eqs. (58)–(60). Thus, if one has accurate frequency response data for these extremes as well as for intermediate frequencies, a good estimate of r may be obtained from fitting, even when r is very large (say $\geq 10^6$). But, of course, the larger r the wider the frequency range required. Alternatively, since r is generally a strong exponential function of T^{-1}, one can often increase T until r is much smaller.

In many cases of interest α and β are likely to be temperature dependent. But whether they are or not, if the DAE model applies, the quantity

$$\ln(r)/\ln(\tau_0/\tau_a) = (\mathscr{E}_\infty/\mathscr{E}_0) - 1 = (E_\infty/E_0) - 1, \tag{61}$$

should be entirely temperature independent. When r and τ_0 estimates are well determined one can test this requirement by ordinary least-squares fitting of τ_0 and r data to the linear equation

$$\ln(\tau_0) = A_5 + B_5 \ln(r), \tag{62}$$

where $A_5 \equiv \ln(\tau_a)$ and $B_5 \equiv E_0/(E_\infty - E_0)$. If fitting with this equation yields reasonable values for τ_a and E_∞/E_0, one can fit the ϕ_C data to $\phi_C = (\alpha - kT\eta)/(\alpha + \beta)$ using the Eq. (46) expressions for α and β. Initially one might set $T_{\infty\alpha} = T_{\infty\beta} = 0$ and $T_{0\alpha} = T_{0\beta} = T_0$ and determine η, T_0, α_0, and β_0 by nonlinear least-squares fitting. The resulting values of $\alpha(T)$ and $\beta(T)$ could then be used with the expressions for τ_0 and r to obtain estimates of E_∞ and E_0.

A statistically more appropriate approach, but a more complicated one, would be to use nonlinear least squares to fit the τ_0, r, and ϕ_C data simultaneously. With the usual

assumption that parameter standard deviations are proportional to parameter magnitudes, one would use weighted nonlinear least squares to minimize the sum of squares:

$$S = \{[1-(r_e/r_t)]^2 + [1-(\tau_{0e}/\tau_{0t})]^2 + [1-(\phi_{Ce}/\phi_{Ct})]^2\}. \quad (63)$$

Here the "e" and "t" subscripts stand for "experimental" and "theoretical," respectively. One would thus obtain estimates of $E_0, E_\infty, \tau_a, \eta, T_{0j}, T_{\infty j}$, and χ_{0j} and their standard deviations, taking all data and interactions into account simultaneously. Only really excellent CNLS fitting results would justify using this complicated approach, however.

ACKNOWLEDGMENTS

The author is grateful to Dr. Stephen W. Kenkel and Mr. Robert L. Hurt for their valuable help and suggestions and to the U. S. Army Research Office for financial support.

APPENDIX A

Here we shall outline the sort of approach used in Refs. 12, 13, and 16 to obtain closed-form expressions from an equation like Eq. (15) with $\tau_{Dx} = \infty$. Although these authors all separated the integral into a real and imaginary part before integrating, this procedure is unnecessary and merely complicates the analysis. Therefore, we shall eschew such separation, as we have done to obtain the exact results listed in Appendix B. This simplification will still allow us to demonstrate the problems in the preceding work and show why its results are inapplicable to the present situation.

Since we will be dealing with unnormalized results here, it will be sufficient to consider just the integral of Eq. (32) for a D system and define

$$J_D \equiv \int_1^r \frac{W^{\phi_D - 1}\, dW}{1 + pW}, \quad (A1)$$

where $p \equiv is$. In agreement with the earlier work we now take $r = \infty$. We may rewrite the resulting integral as

$$^{\infty}J_D \equiv {}^{\infty}J_{D\infty} - J_{D1} \equiv \int_0^{\infty} \frac{W^{\phi_D - 1}\, dW}{1 + pW} - \int_0^1 \frac{W^{\phi_D - 1}\, dW}{1 + pW}. \quad (A2)$$

Although the earlier workers took $\tau_0 \equiv 0$, we need not make this assumption here since τ_0 only appears in the definition of p and scales the frequency variable.

Expressed in the present notation the earlier workers assumed that $^{\infty}J_D \cong {}^{\infty}J_{D\infty}$ for $sW \ll 1$ and thus implicitly neglected J_{D1}. But $sW = \omega\tau_a e^{\gamma\vartheta} = \omega RC$, and if the upper limit of r is ∞, the $sW \ll 1$ condition cannot be satisfied for nonzero s when $\gamma > 0$. There is therefore no finite frequency range over which $^{\infty}J_{D\infty}$ is a good approximation to $^{\infty}J_D$. Let us continue the analysis, however, along the lines followed by the earlier workers. The integral $^{\infty}J_{D\infty}$ may be considered a Mellin transform and is readily evaluated to yield

$$^{\infty}J_{D\infty} = (is)^{-\phi_D}\pi \csc(\pi\phi_D) \quad (A3)$$

for $0 < \phi_D < 1$, quite different from our present $I_D(\phi_D)$ DAE results. Now it is easy to show for $s = 0$ that the basic integral of Eq. (A1) only converges for $\phi_D < 0$ when $r = \infty$. This is another example of inconsistency arising from the $r = \infty$ choice together with the use of $^{\infty}J_{D\infty}$.

Now the admittance associated with $^{\infty}J_{D\infty}$ is proportional to $[(is)\,{}^{\infty}J_{D\infty}]$ which we may define as

$$^{\infty}K_{D\infty} \equiv (is)^{1-\phi_D}\pi \csc(\pi\phi_D). \quad (A4)$$

For the dielectric case considered earlier,[12,13,16] we have defined $\psi_D \equiv 1 - \phi_D$. Here $\psi_D = (\alpha + \lambda)/(\alpha + \beta)$, and $\beta = 0$, $\alpha = 1$, and $\lambda < 0$ were assumed in Refs. 12 and 13, while λ was implicitly taken zero in Ref. 16. Now we may write

$$^{\infty}K_{D\infty} = (is)^{\psi_D}\pi \csc(\pi\psi_D) = (\pi/2)s^{\psi_D}[\csc(\psi_D\pi/2) + i\sec(\psi_D\pi/2)], \quad (A5)$$

essentially the result of Refs. 12, 13, and 16. Very nearly this same result was also given long ago (Ref. 11, Table I, line 4). This equation shows the same ω^n frequency dependence as the CPE of Eq. (3) and, in addition involves real and imaginary parts which are properly related by the Kronig–Kramers requirement,[11] $\mathrm{Im}(^{\infty}K_{D\infty}) = \mathrm{ctn}(\psi_D\pi/2)\,\mathrm{Re}(^{\infty}K_{D\infty})$. But the presence of the $\csc(\pi\psi_D)$ term precludes full identification of the above result with the CPE as written in its usual form [Eq. (3)]. When a new normalized frequency variable $s_n \equiv s[\csc(\pi\psi_D)]^{1/\psi_D}$ is defined, however, Eq. (A5) is of just the CPE form in terms of this new frequency variable. In spite of the complete inapplicability of the present result, it does lead to ω^{ψ_D} frequency response (if it actually applied for $\omega > 0$) of the same general form predicted by the exact analysis over a limited, finite range of ω.

Now one may ask whether it is possible to obtain frequency response of the form of Eq. (2), with $1 < n < 2$, from any of the foregoing analyses. The theoretical work of Dutoit *et al.*[12] is for a D system and does not lead directly to the constant b term of Eq. (2). A resistor in series with the D-system impedance is needed to provide this term; the resulting response is then not that of a general D system. Although Dutoit *et al.*[12,13,42] showed that their theory, which we have seen is not actually applicable, could lead to a ω^{-n} term in $\mathrm{Re}(Z)$ with $1 < n < 2$, this result required the implausible assumption $\lambda < 0$ and the neglect of the frequency dependence of the capacitance associated with the total admittance. Thus, these theoretical results cannot be accepted as an adequate explanation of the experimental behavior.

What of the predictions of the present DAE theory? The results of Table IV for T_D show that an ideal D system by itself will not lead to $n > 1$ response for $\mathrm{Re}(Z)$. Here T_D is the impedance function. But if $\epsilon_\infty \gg (\epsilon_0 - \epsilon_\infty)$, so that ϵ_∞ dominates in ϵ', it follows that the exponents of T'_D and T''_D in the intermediate frequency range are approximately $-(1 + \psi_D)$ and -1, respectively. Thus with $\psi_D > 0$, it is possible to obtain $n > 1$ response. Since here $\psi_D \equiv (\alpha + \lambda)/(\alpha + \beta)$, such response does not necessarily require $\lambda < 0$. On the other hand, the results of Table IV show that the impedance function in the C-system case I_C can directly involve an I'_C exponent greater than unity. In order to obtain such response, however, it is necessary that $\phi_C \equiv (\alpha - \lambda)/(\alpha + \beta)$ be greater than unity. Although this is possible if $\lambda < 0$, this condition is unlikely. But as we have seen, β may be negative. For example, if $\alpha = 1$ and $\beta = -0.5$, $\phi_C = 2 - 2\lambda$, which

leads to $\phi_C \leqslant 2$ for positive λ. More detailed fitting of experimental results such as those of Ref. 12, especially on data obtained for two or more different temperatures, would be needed to allow one to choose unambiguously which of the D- or C-system responses is the more appropriate.

APPENDIX B

We list here exact closed-form results for $I_i(\phi_i)$ [Eq. (32)] for various ϕ_i choices. From these results Y_{DNN} and Y_{DN} and Y_{CNN} and Y_{CN} expressions can be readily obtained.

$$I_i(1.5) = (3/is)\left[(\sqrt{r}-1)/(r^{3/2}-1)\right]\left[1 - I_i(0.5)\right]; \quad \text{(B1)}$$

$$I_i(1) = (1/is)(r-1)^{-1}\ln\left[(1+isr)/(1+is)\right]; \quad \text{(B2)}$$

$$I_i(2/3) = \left[3(is)^{2/3}(r^{2/3}-1)\right]^{-1}\left[T - L\right]; \quad \text{(B3)}$$

$$I_i(0.5) = \left[\sqrt{is}(\sqrt{r}-1)\right]^{-1}\tan^{-1}\left(\frac{\sqrt{is}(\sqrt{r}-1)}{1+is\sqrt{r}}\right); \quad \text{(B4)}$$

$$I_i(1/3) = \left[6(is)^{1/3}(r^{1/3}-1)\right]^{-1}\left[T + L\right]; \quad \text{(B5)}$$

$$I_i(0) = \ln\left[r(1+is)/(1+isr)\right]/\ln(r); \quad \text{(B6)}$$

and

$$I_i(-0.5) = 1 - (is\sqrt{r})I_i(0.5), \quad \text{(B7)}$$

where

$$L \equiv \ln\left[\left(\frac{1+(isr)^{1/3}}{1+(isr)^{1/3}}\right)^2\left(\frac{1-(is)^{1/3}+(is)^{2/3}}{1-(isr)^{1/3}+(isr)^{2/3}}\right)\right] \quad \text{(B8)}$$

and

$$T \equiv 2\sqrt{3}\tan^{-1}\left(\frac{(\sqrt{3}/2)(is)^{1/3}(r^{1/3}-1)}{1-0.5(is)^{1/3}(r^{1/3}+1)+(is)^{2/3}r^{1/3}}\right). \quad \text{(B9)}$$

Care was necessary in the numerical evaluation of the $\tan^{-1}$ of a complex argument. Because of the multiple-value property of tan, it was necessary to add π to the $\tan^{-1}$ function of Eq. (A9) whenever it yielded a negative real part. Incidentally, the first quadrant roots of $(i)^{1/2}$ and $(i)^{1/3}$ were used throughout. The above formulas have been verified by direct numerical integration.

There are two limiting conditions which the above results must satisfy. First, they must all reduce to $I_i(s,\phi_i) = 1$ for $s = 0$ and any ϕ_i and r. Second, when $r \to 1$, $F_i(E)$ becomes a δ function[8,11] involving $\delta(W-1)$, and all I_i's should reduce to just

$$I_i \to (1+is)^{-1}, \quad \text{(B10)}$$

simple single-time-constant Debye dispersion. Both conditions are satisfied by all the above expressions. Some of the above formulas derived for I_D only and with a less general definition of ψ_D appear in Ref. 17. These authors did not realize that for most of their ψ_D values the $r \to \infty$ limit does not lead to measurable results. Their expressions were derived only for a DRT while those given here apply to both a DRT and a DAE.

[1] M. Gevers and F. K. du Pré, Trans. Faraday Soc. **42A**, 47 (1946).
[2] C. G. Garton, Trans. Faraday Soc. **42A**, 56 (1946).
[3] J. R. Macdonald, J. Chem. Phys. **36**, 345 (1962).
[4] K. S. Cole and R. H. Cole, J. Chem. Phys. **9**, 341 (1941).
[5] D. W. Davidson and R. H. Cole, J. Chem. Phys. **19**, 1484 (1951).
[6] A. S. Nowick and B. S. Berry, IBM J. Res. Dev. **5**, 297 (1961).
[7] J. R. Macdonald, Physica **28**, 485 (1962).
[8] J. R. Macdonald, J. Chem. Phys. **40**, 1792 (1964).
[9] J. R. Macdonald, J. Appl. Phys. **34**, 538 (1963).
[10] N. Alberding, R. H. Austin, S. S. Chan, L. Eisenstein, H. Frauenfelder, I. C. Gunsalus, and T. M. Nordlund, J. Chem. Phys. **65**, 4701 (1976). See also R. H. Austin, K. W. Beeson, L. Eisenstein, H. Frauenfelder, and I. C. Gunsalus, Biochemistry **14**, 5355 (1975), and P. G. Debrunner and H. Frauenfelder, Annu. Rev. Phys. Chem. **33**, 283 (1982).
[11] J. R. Macdonald and M. K. Brachman, Rev. Mod. Phys. **28**, 393 (1956).
[12] E. C. Dutoit, R. L. Van Meirhaeghe, F. Cardon, and W. P. Gomes, Ber. Bunsenges. Phys. Chem. **79**, 1206 (1975).
[13] W. H. Laflère, R. L. Van Meirhaeghe, F. Cardon, and W. P. Gomes, Surf. Sci. **59**, 401 (1976).
[14] J. R. Macdonald, Solid State Ion. **13**, 147 (1984).
[15] J. Keilson, *Markov Chain Models—Rarity and Exponentiality* (Springer Berlin, 1979), Applied Mathematical Sciences, Vol. 28.
[16] J. F. McCann and S. P. S. Badwal, J. Electrochem. Soc. **129**, 551 (1982).
[17] A. Matsumoto and K. Higasi, J. Chem. Phys. **36**, 1776 (1962).
[18] C. J. F. Böttcher and P. Bordewijk, *Theory of Electric Polarization*, Vol. II (Elsevier, New York, 1978) Chap. IX.
[19] H. Engstrom, J. B. Bates, and J. C. Wang, Solid State Commun. **35**, 543 (1980).
[20] J. R. Macdonald, J. Schoonman, and A. P. Lehnen, Solid State Ion. **5**, 137 (1981).
[21] S. P. S. Badwal and H. J. de Bruin, Aust. J. Chem. **31**, 2337 (1978).
[22] C. Ho, I. D. Raistrick, and R. A. Huggins, J. Electrochem. Soc. **127**, 343 (1980).
[23] J. Schoonman, L. J. Stil, J. R. Macdonald, and D. R. Franceschetti, Solid State Ion. **3/4**, 365 (1981).
[24] J. R. Macdonald, A. Hooper, and A. P. Lehnen, Solid State Ion. **6**, 65 (1982).
[25] J. R. Macdonald, J. Schoonman, and A. P. Lehnen, J. Electroanal. Chem. **131**, 77 (1982).
[26] Y.-T. Tsai and D. H. Whitmore, Solid State Ion. **7**, 129 (1982).
[27] S. P. S. Badwal, J. Electroanal. Chem. **161**, 75 (1984).
[28] J. R. Macdonald and G. B. Cook, J. Electroanal. Chem. (in press)
[29] S. P. S. Badwal, J. Mater. Sci. **19**, 1767 (1984).
[30] J. R. Macdonald and C. A. Hull, J. Electroanal. Chem. **165**, 9 (1984).
[31] D. Ravaine and J.-L. Souquet, C. R. Acad. Sci. Ser. C **277**, 489 (1973).
[32] J. R. Macdonald, in *Superionic Conductors*, edited by G. D. Mahan and W. L. Roth (Plenum, New York, 1976), p. 81. See also J. R. Macdonald, Solid State Ion. **15**, 159 (1985).
[33] D. R. Franceschetti and J. R. Macdonald, J. Electroanal. Chem. **101**, 307 (1979).
[34] J. Schrama, Thesis, Leiden, The Netherlands, 1957, pp. 114–120 (unpublished).
[35] D. R. Franceschetti and J. R. Macdonald, J. Electrochem. Soc. **129**, 1754 (1982).
[36] G. Williams and D. C. Watts, Trans. Faraday Soc. **66**, 80 (1970).
[37] G. Williams, D. C. Watts, S. B. Dev, and A. M. North, Trans. Faraday Soc. **67**, 1323 (1970).
[38] M. F. Shlesinger and E. W. Montroll, Proc. Nat. Acad. Sci. **81**, 1280 (1984).
[39] E. W. Montroll and J. T. Bendler, J. Stat. Phys. **34**, 129 (1984).
[40] C. T. Moynihan, L. P. Boesch, and N. L. Laberge, Phys. Chem. Glasses **14**, 122 (1973).
[41] S. W. Kenkel (unpublished).
[42] W. H. Laflère, R. L. Van Meirhaeghe, and F. Cardon, Surf. Sci. **74**, 125 (1978).